eprints@whiterose.ac.uk
https://eprints.whiterose.ac.uk/

Supercritical Carbonation of Lightweight Aggregate Containing Mortar: Thermal Behavior

MARÇAL Rosas Florentino Lima Filho[1,a], SANDRO Marden Torres[1,b], LEON Black[2,c] , ANDRESSA de Araújo Porto Vieira[1,d], RODINEI Medeiros Gomes[1,e] and KELLY Cristiane Gomes[1,f]

[1]Universidade Federal da Paraíba, UFPB/CT Campus Universitário sn 50051-900 João Pessoa – PB, Brazil
[2]The University of Leeds, School of Civil Engineering, Leeds, LS2 9JT

[a]marcal_civil@yahoo.com.br, [b]sandro.marden@pq.cnpq.br, [c]l.black@leeds.ac.uk, [d]andressa.pv@hotmail.com, [e]gomes@lsr.ufpb.br, [f]gomes@cear.ufpb.br

Abstract. Lightweight concrete shows good insulation properties, depending on several parameters such as mix design and aggregate type. Perlite aggregate is one of the most effective aggregates for such a purpose, mainly because of its low thermal conductivity (0.04 W/m.^{o}C), but is not available globally. This paper explores the potential use of another source of thermal efficient aggregate, vermiculite (0.058 W/m.^{o}C) which is available in Brazil and other countries where perlite is absent. Cylindrical samples were cast by using two lightweight aggregates, perlite and vermiculite, and treated with supercritical carbon dioxide. Supercritical carbonation (SCC) of concrete can improve mechanical, thermal and durability features. In this paper, the effect of SCC on the thermal behavior of lightweight mortars was investigated with regards to physical and microstructure features and thermal behavior due to cooling.

Introduction

Lightweight concrete produced with lightweight aggregates, as perlite or vermiculite, is used for many applications, such as filling and regularization of slabs, floors and ceiling elements. It shows improved thermal/acoustic behaviour and resistance to freeze-thawing cycles than normal weight concrete, but it has the disadvantage of low compressive strength and durability [1-4].

Perlite is a siliceous volcanic glass, the volume of which can increase substantially under the action of heat, exhibiting a 4-20 fold volume increase when heated above 870°C [5]. As a result of this volume increase and its porous structure, the water absorption of expanded perlite is significant. Furthermore, since its density is very low, expanded perlite shows exceptional thermal insulation properties. Despite its thermal properties, natural sources of perlite comprise only few countries (Mexico, United State, China, Greece, Japan, Italy and Turkey).

Vermiculite is natural clay constituted of hydrated silicate with magnesium, aluminium and iron in its structure that also shows similar thermal properties. It can also be expanded to similar volume increase order as perlite. Alongside the main producers of perlite, it is also found in other countries such as Brazil (10% of resources and 4th place in production worldwide), India and South Africa, and the Paraiba state been one of its main producers.

Table 1 shows thermal property values of the main aggregates used to produce lightweight concrete [6, 7]. One of the lowest values of thermal conductivity is perlite, followed by vermiculite and limestone. This carbonate phase has lower thermal conductivity values when compared to quartz.

Table 1: Some Typical Thermal Properties of Concrete Phases.

	Specific Heat Capacity	Thermal Conductivity
	C (J/kg.K)	W/m.K
Concrete	0.96	0.80
Limestone/Calcite	0.84	1.26
Quartz	0.80	3.00
Perlite	0.84	0.04
Vermiculite	0.84	0.06
Air	1.01	0.03

Supercritical carbonation is a process in which carbon dioxide is in a supercritical state (temperature > 31.6°C and pressure > 73 bar). In such condition, CO_2 is considered as a solvent, with a liquid-like density and gas-like transport properties [8]. Under these conditions, carbonation of cement pastes takes hours instead of years [9]. In that sense, supercritical carbonation can act as a pore reducing agent in cement paste with the conversion of calcium hydroxide into the more stable calcium carbonate, yielding to changes in the pore structure of cement matrices [10-14]. Nonetheless, very few studies address the issue of interfacial transition zone between cement paste and aggregates, especially taking into consideration the nature of the porosity of each lightweight aggregate. Indeed, both expanded perlite and vermiculite not only presents distinct intrinsic microporosity but different chemical composition. This paper aims to evaluate whether the SCC affects the thermal behaviour of lightweight, exploring the potential use of another source of thermal efficient aggregate (expanded vermiculite) as an alternative lightweight aggregate for mortars.

Materials and Methods

Cylindrical samples (50 mm diameter, 40 mm deep) were hand compacted and cast according to the composition shown in Table 1. The samples were cured in fog room at ambient temperature (around 20°C for 28 days prior to testing).

Table 2: Mix parameters of mortar cylinders.

Mix	Cement	Aggregate	Curing Regime	Volume Fraction
1		Quartzite Sand		
2	CEM I 52.5 R	Perlite	28 days in fog room	1:3
3		Vermiculite		

Visual Assessment: After curing, the samples were oven dried for 48 hours at 40 ± 2 °C (which was shown to lead to constant weight), and then cut. A visual assessment was performed by recording digital images of the cross section to reveal both the center and the edge.

Microstructure: Samples were resin impregnated, then polished to reveal smooth cross-sections. Microstructures were then viewed using a backscattered electron detector.

Supercritical Carbonation: Before the supercritical carbonation process, the samples were oven dried for 48 hours at 40 ± 2 °C. Six samples treated simultaneously, by pumping liquefied compressed CO_2 at a rate of ~10 ml min^{-1} into a temperature-controlled stainless steel vessel for approximately an hour until the temperature and pressure reach 40 °C and 100 ± 1 bar respectively. The flow was then decreased to ~1 ml min^{-1} to compensate for any pressure loss, and monitored for more 4 hours. The samples then remained in the chamber for a further 43 hours, making 48 hours in total.

Bulk Density Determination: Water Vacuum Saturation Test was based on ASTM C 1202 [6] and described by Safiuddin [7]. Three samples (pre- and post-carbonation) were removed from curing at 7 and 28 days, then oven dried at 40±2ºC to constant mass. The specimens were weighed to prior to saturation, and placed in a desiccator under vacuum for 3 h at 90 kPa, after which the vacuum pump was closed and the samples immersed in cooled boiled water. With the samples covered with water, the vacuum was applied again for a further 1 hour. Air was then allowed to enter and the samples were soaked under water for 20 hours. The saturated surface mass and the buoyant mass were determined, with the permeable porosity calculated by weighting the samples under water and using the Archimedes principle:

$$P_p = \frac{W_s - W_d}{W_s - W_b} \qquad (1)$$

W_b = sample saturated buoyant mass in water;
W_d = sample oven-dry mass in air;
W_s = sample saturated surface-dry mass in air;

Helium Gas Pycnometer Test: Samples of oven-dried raw and SCC treated mortar, were cut into small pieces and placed in a Quantachrome Helium Ultrapycnometer 1000 (resolution of 0.001g/cm3). By using the Archimedes displacement principle and measuring the difference between specific and bulk volumes of a sample material density could be determined [17-19]. The density of the material is then equal to the sample volume minus the gas volume difference between empty and filled camera over mass.

$$\rho_N = \frac{100(\rho_g - \rho_l)}{\rho_g} \qquad (2)$$

ρ_N = Normalized Bulk Density;

ρ_g = Helium Gas Determined Bulk Density;

ρ_l = Water Determined Bulk Density;

ρ_{NSCC} = Normalized Bulk Density after Supercritical Carbonation using Eq. 2.

Thermal Behavior Assessment: Oven-dried cylinders, both pre- and post-carbonation, were put in an oven for 48 hours at 40 ± 2ºC until they reached a stable temperature. After this period they were removed from the oven and left in a lab environment, at room temperature, and imaged at 1, 4, 9, 16, 25, 36, 49, 64 minutes using a FLUKE thermal camera (thermal sensitivity ± 0.09 ºC at 30ºC, temperature range: -20ºC to 150ºC) using the infra-red principle. The images were interpreted by considering the temperature distribution profile, using the SMARTVIEW^{TM} software. The relative specific heat variation was calculated according to Equation 3. The curve of each cooling profile was fit to the Newton's cooling law as shown in Equation 4.

$$c = \frac{Q}{m(T_0 - T_{(t)})} \qquad (3)$$

$T_0 = 50ºC$
Q=constant
c= specific heat;
m= mass;
$T_{(t)}$= Temperature at t seconds

$$T_{(t)} = T_{equ} + (T_0 - T_{equ})e^{-kt} \qquad (4)$$

$T_{(t)}=$ Temperature at t seconds;
$T_0=$ Initial temperature ($\sim$50°C);
$T_{equ}=$ Equilibrium temperature;
t= Time in seconds;
k= *Newton's cooling constant*

Results

Visual Assessment:

Figure 1 shows cross-sectioned edges of the different mortars after 28 days of fog curing, prior to SCC.
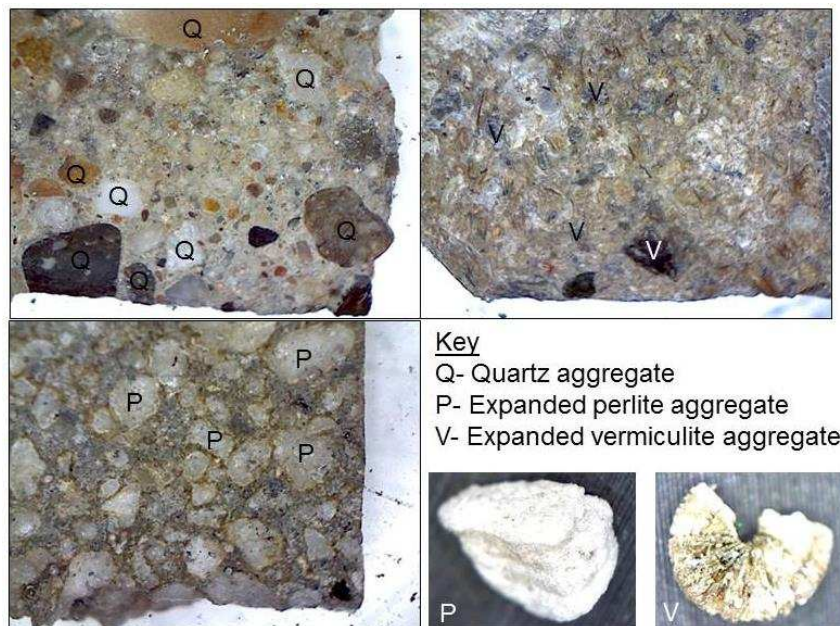
Figure 1: Cross section overview of mortars after 28 days of curing.

The mortars containing lightweight aggregates (P and V) presented similar features to the control mortar with quartz, with similar distributions of particles within the cement matrix. Although their shapes and sizes were similar, both lightweight aggregates presented rough surface textures. Despite this, the mortars appeared sound, with the cement matrix surrounding the grains and no evidence macro porosity or cracking was observed.

Microstructure:

Figure 2 shows the microstructures of the three mixes after 28 days of curing in fog room, prior to SCC.
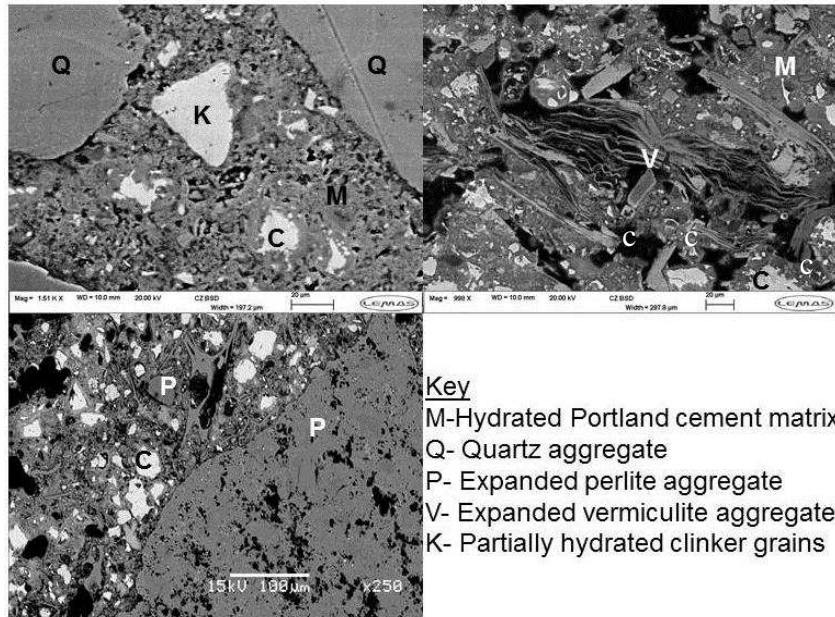
Figure 2: Polished Surface Backscattered Electron Image Micrograph of mortars.

The microstructure of quartz-containing mortar was typical of a Portland cement mortar, with sound aggregate grains embedded in a slightly porous matrix comprising hydrated cement paste (HCP) plus some residual anhydrous cement clinker. The interfacial transition zone (ITZ) was consistent across the sample. The microstructures of both lightweight aggregate samples however presented very different porous structures. The perlite-containing mortar exhibited intra-aggregate porosity and considerable porosity within the HCP, but with a well-defined ITZ. The vermiculite-bearing mortar meanwhile showed an inter-lamellar porosity, which allowed some cement hydrated phases to intrude inside the aggregate itself (designated 'c' in Figure 2), thus disrupting the ITZ.

Supercritical Carbonation:

Figure 3 shows external and cross-sectioned views of the mortars subjected to supercritical carbonation after having been sprayed with phenolphthalein.
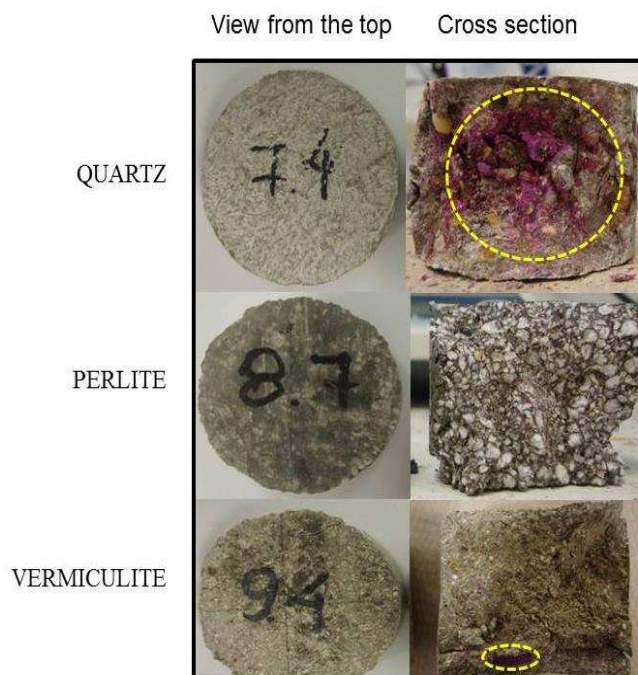
Figure 3: Phenolphthalein Sprayed Mortar samples after Supercritical Carbonation.

The level of carbonation varied between samples, and whilst all samples retained a small amount of uncarbonated material, carbonation was far more pronounced in the lightweight mixes. The quartz-containing samples showed the least carbonation, which remained superficial, as demonstrated by the pink color evident within much of the bulk of the sample. Although carbonation was very intense in vermiculite samples, it was not as complete as in perlite samples, as shown by the presence of some alkaline areas (assigned as dashed line in the bottom right - Figure 3).

Bulk Density Assessment:

Figure 4 shows the variation in bulk density as determined by helium pycnometry and water immersion for the three mixes, both pre- and post-carbonation.
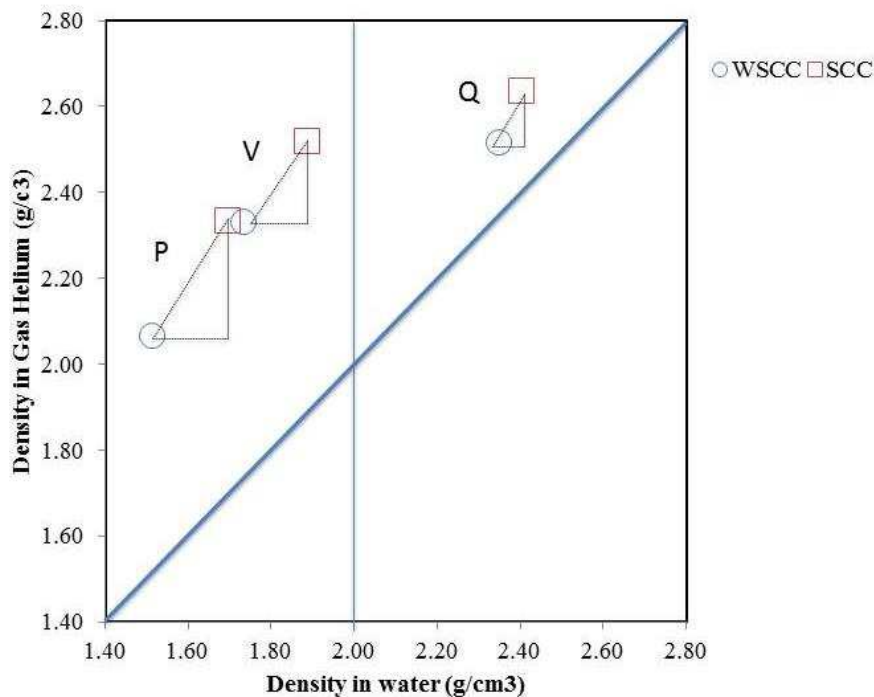
Figure 4: Helium (left) and water (right) bulk density of Mortar samples before and after Supercritical Carbonation.

It can be observed that SCC led to a clear increase in density for all mixes, being greatest for perlite, followed by vermiculate and finally quartz. Mixes with vermiculite and perlite can be categorized as lightweight mortars as their densities fall below 2.0 g/cm^3 [20,21], even after supercritical carbonation. The increases in density correlated with the degree of carbonation determined by spraying with phenolphthalein. The increases in density were more pronounced when determined by gas than by water in all cases. This indicates that the porous system has different ranges, in which the smaller range can be mainly assessed only by the gas ability to penetrate in smaller pores.

Normalizing density according to the gas density (Eq. 2) demonstrates that the quantity of pores inaccessible to water was far greater for lightweight aggregates (ρ_N P=27% and ρ_N V=26%) than for quartz aggregate (ρ_N Q=9%), reflecting the intra-aggregate porosity of the lightweight samples. Nevertheless, supercritical carbonation had little effect on the percentage of pores inaccessible to water; with an increase of just a few percent (ρ_{NSCC^-} ρ_N P=4%, ρ_{NSCC^-} ρ_N V=1% and ρ_{NSCC^-} ρ_N Q=3%).

Thermal Behavior Assessment:

Figure 6 presents the temperature profile across the cross section at the beginning and end of the evaluated period, before and after supercritical carbonation for different types of aggregates.
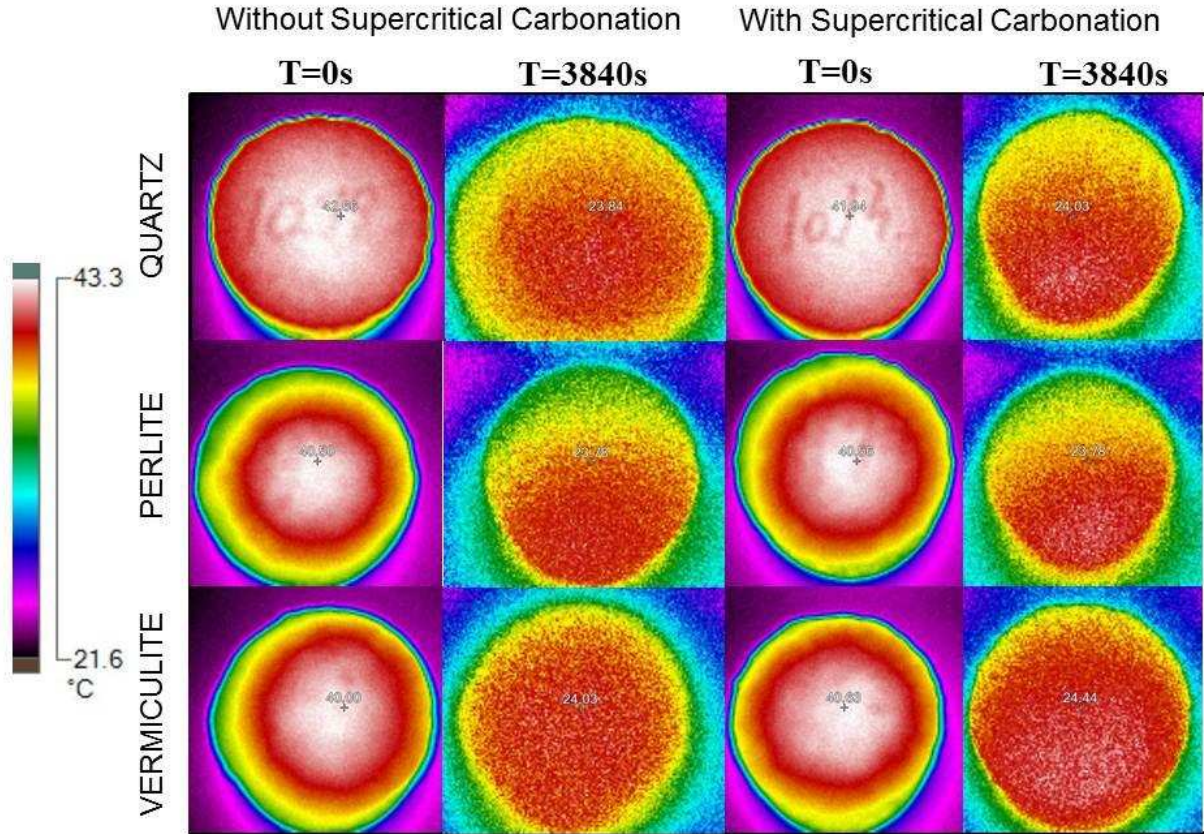
Figure 6: Superficial Temperature profile with time of Mortar samples before and after Supercritical Carbonation.

During the first stage of cooling, the temperature profile across the cross section was greatly affected by the type of aggregate. Whereas a similar rate of cooling was found across the surface of the reference mortar, the porous aggregate containing systems tended to have lower surface temperatures. This was characterized by the formation of successive temperature halos in lightweight aggregate samples, but not in quartz containing mortars. After a long period of cooling, all samples showed a more homogeneous temperature profile, despite the type of aggregate.

The effect of supercritical carbonation was not qualitatively detected as it did not have a significant thermal contrast image in the camera. Nevertheless, the actual effect can be easily seen when the temperature is quantitatively evaluated as shown in Figure 7.
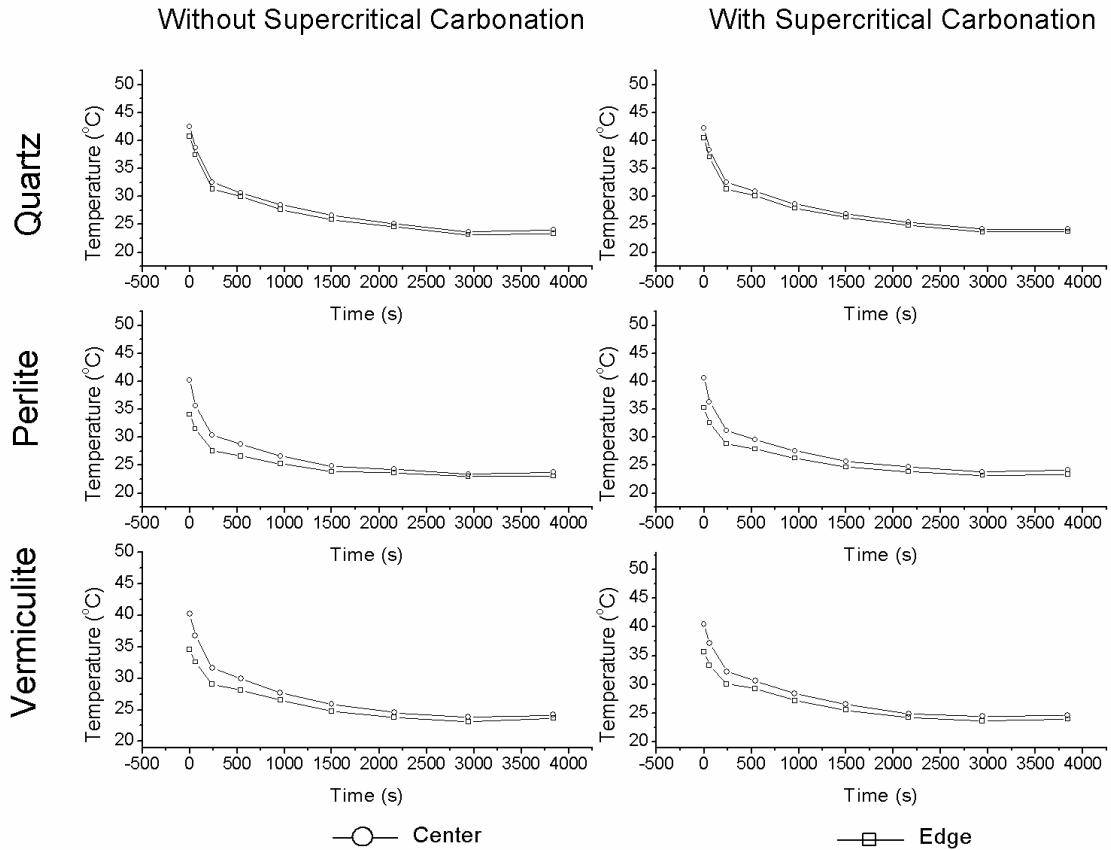
Figure 7: Superficial Temperature cooling profile with time of Mortar samples before and after Supercritical Carbonation.

All samples presented similar cooling profiles, following an exponential decay trends. The initial temperatures were always lower for the lightweight mortars than observed in the reference quartz aggregate system, indicating the former absorbed less heat than the latter. This can be related to a lower capacity for storing thermal energy by the porous aggregate containing systems. Furthermore, despite all mixes having been subjected to the same heat and time, whilst the edge and center temperatures of the reference mortar were the same, the initial edge temperatures of the lightweight mortars were more than five degrees lower than the center. This reflects the different heat capacities of each system.

Figure 8 shows the variation of relative specific heat and time, admitting a constant energy supplied by the source.
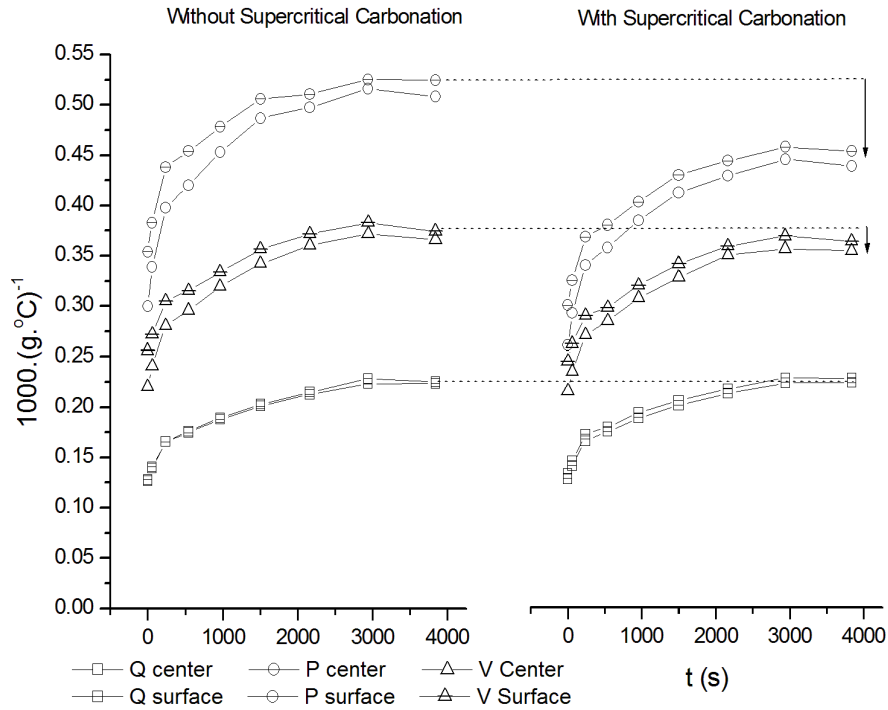
Figure 8: Superficial Temperature cooling profile with time of Mortar samples before and after Supercritical Carbonation.

Supercritical carbonation reduces the relative specific heat for lightweight aggregates but not for the quartz samples. The intensity of such reduction is clearer in perlite samples but also evident in vermiculite. The border effect still persists for the lightweight samples. The difference in such reduction for lightweight samples can be associated with the precipitation of carbonate phases and the differences in each ITZ (as shown in microstructure section).

Table 4 shows the Newton´s cooling constant and parameters of all mixes, considering the thermal profile as observed in Figure 6 and plotted in Figure 7. Before SCC , the cooling rate (K) showed little difference between Q and V, but was higher in P. Despite being always lower at the edge, the difference between the cooling rate at the center and the edge ($K_{Center-edge}$) was small for P and Q but slightly greater for V.

In general, SCC reduced the average Newton´s constant of cooling (K_{med}) of all aggregates. Such reduction was more pronounced for the lightweight aggregates, especially perlite, but there was very little effect for the quartz samples.

Characterized by the differences between (i) the cooling rate and (ii) the temperature at the center and the edge of the samples (as shown in Figures 6 and 7), the edge effect was magnified by SCC for the lightweight samples.

Table 4: Newton´s cooling constants and parameters of mortar before and after Supercritical Carbonation.

Mix	K				Initial T		
	Center	Edge	kmed	Delta K	Center	Edge	Delta T
Q	0.00204	0.00198	0.00201	0.6	41.1	39.5	-1.7
QCc	0.00198	0.00198	0.00198	0.0	40.7	39.1	-1.6
P	0.00276	0.00267	0.00272	1.0	38.9	33.4	-5.6
PCc	0.00237	0.00192	0.00215	4.5	39.2	34.2	-5.0
V	0.00204	0.00161	0.00183	4.3	39.0	33.7	-5.3
VCc	0.00185	0.00140	0.00163	4.6	39.2	34.6	-4.6
Q-QCc	3%	0%	1%				
P-PCc	14%	28%	21%				
V-Vv	9%	13%	11%				

General Remarks

Despite a visual examination of cross-sectioned mixes showing similar features with no apparent macroporosity or crack systems, the microstructure of the lightweight aggregate containing mortars showed rather different types of microporosity: (i) interconnected pores within the cement matrix and cement-aggregates interface; (ii) intra-grain self-contained porosity in perlite and (iii) an inter-lamellar porosity in vermiculite. The lamellar porosity in the vermiculite sample interfered with the ITZ. There were no hydrated cement products observed within the large grains of both perlite and quartz but at the cement matrix and cement-aggregates interface.

Visual evaluation via Phenolphthalein test gave evidence that SCC occurred from the surface inwards, most evidently in quartz samples. Little or no evidence of residual alkaline areas was detected in lightweight aggregates, confirming their open pore microstructure.

The differences between gas and water bulk density measurements were much greater for both lightweight aggregate after SCC (greater than 26%). Indeed, the conversion of calcium hydroxide to calcium carbonate can only result in an increase in density of c.a. 18% to 31% ($\rho_{portlandite}$=2.23g/cm^3; $\rho_{calcite}$=2.71g/cm^3; $\rho_{vaterite}$=2.64g/cm3; $\rho_{aragonite}$=2.94g/cm^3; $\rho_{calcite}$=2.71g/cm^3) [ref]. Nonetheless, only small differences were observed in the increase of the normalized bulk density for all aggregates due to SCC (ρ_{NSCC}- ρ_N P=4%, ρ_{NSCC}- ρ_N V=1% and ρ_{NSCC}- ρ_N Q=3%). So, the latter gives evidence that the effect of SCC was more detectable within the water permeable porosity. This can be an indication that the supercritical carbonation process mostly affects the porosity range detectable by water, even though the CO_2 transport properties are considered to be of those of a gas like state and its density of those of a liquid like state [ref].

As far as thermal behavior is concerned, the temperature homogeneity throughout the cross section is greatly affected by the type of aggregates. Whereas similar rate of cooling were found in control samples across the surface, systems containing porous aggregate tended to have lower rates of cooling at the edges. The edge effect might be associated with: (i) differences in the porosity between the control and the lightweight containing aggregates; (ii) lower thermal conductivity of porous aggregates and (iii) the precipitation of phases with lower thermal conductivity within the porous structure (Air-0.026 W/m.^{o}C and calcium carbonates-1.0 W/m.^{o}C).

Conclusions

SCC is responsible for the increase in density of all mortars, more so in lightweight aggregate containing samples. In the porous aggregate systems, SCC affects the thermal behavior of the mortars depending on the lightweight aggregate microstructure. As shown by microstructure assessment, HCP can form within the vermiculate aggregates but not in perlite or quartz. Because quartz presents a more compact microstructure, and hence less air, the effect of SCC is mainly within the matrix. Perlite mortars showed an enclosed porosity within the aggregate and also larger pore size distribution. Vermiculite-containing mortars were characterized by an intra-lamellar structure, hence, allowing the precipitation of cement hydrates and carbonates within its structure. The Newton´s cooling parameters suggest that SCC decreases the heat transfer from the center to the edge during cooling only for porous aggregates during the cooling period. This effect is due to the precipitation of lower thermal conductivity carbonate phases within the pore structure.

Acknowledgements

References

[1] R. Dermirboga, I. Orung, R. Gul , Effects of expanded perlite aggregate and mineral admixtures on the compressive strength of low-density concretes, Cement and Concrete Research. 31 (2001) 1627-1632.

[2] O. Unal, T. Uygunoglu , A. Yildiz, Investigation of properties of low-strength lightweight concrete for thermal insulation, Building and Environment. 42 (2007) 584 – 590.

[3] O. Sengul, S. Azizi, F. Karaosmanoglu, M.A. Tasdemir, Effect of expanded perlite on the mechanical properties and thermal conductivity of lightweight concrete, Energy and Buildings. 43 (2011) 671 – 676.

[4] I. Türkmen, A. Kantarci, Effects of expanded perlite aggregate and different curing conditions on the physical and mechanical properties of self-compacting concrete, Building and Environment. 42 (2007) 2378 – 2383.

[5] S. Chandra, L. Berntsson, Lightweight Aggregate Concrete, Noyes Publications/William Andrew Publishing. (2002) 367.

[6] Ozkan, Sengula et al, Effect of expanded perlite on the mechanical properties and thermal conductivity of lightweight concrete, Energy and Buildings. 43 (2011) 671–676.

[7] I.B. Topçu, B. Isikdag, Manufacture of high heat conductivity resistant clay bricks containing perlite. Building and Environment. 42 (2007) 3540 – 3546.

[8] C.L. Page, N.R. Short, P. Purnell, Preliminary investigation into the supercritical carbonation of cement pastes, Journal of Materials Science. 36 (2001) 35 -41.

[9] L. Fernandez-Carrasco, J. Rius, C. Miravitlles, Supercritical carbonation of calcium aluminate cement, Cement and Concrete Research. 38 (2008) 1033-1037.

[10] N.R. Short, P. Purnell, C.L. Page, Preliminary investigation into the supercritical carbonation of cement pastes, Journal of Materials Science. 36 (2001) 35 -41.

[11] L. Black, C. Breen, J. Yarwood, K. Garbev, P. Stemmermann, B. Gasharova, Structural features of C-S-H(I) and its carbonation in air – A Raman spectroscopic study. Part II: carbonated phases, Journal of the American Ceramic Society. 90 (2007) 908-917.

[12] C.A. Garcia-Gonzalez, A. Hidalgo, A. Andrade, M.C. Alonso, J. Fraile, A.M. Lopez-Periago, C. Domingo, Modification of Composition and Microstructure of Portland Cement Pastes as a Results of Natural and Supercritical. 2006.

[13] M.R.F. Lima Filho, L. Black, S.M. Torres. Microstructure of Portland Cement Based Composites under Cryogenic Temperatures, 31 Cement and Concrete Science Conference. 1 (2011) 1-5.

[14] M.R.F. Lima Filho, L. Black , S.M. Torres, The effect of supercritical carbonation on lightweight concrete for natural gas storage, 32 Cement and Concrete Science Conference. 1 (2012).

[15] ASTM C 1202, Standard Test method for electrical indication of concrete's ability to resist chloride ion penetration, in: Annual Book of ASTM Standards, vol. 04.02, American Society for Testing Materials, Philadelphia (2002).

[16] Md. Safiuddin, N. Hearn, Comparison of ASTM saturation techniques for measuring the permeable porosity of concrete, Cement and Concrete Research. 35 (2005) 1008 -1013.

[17] J.G. Cabrera, C.J. Lynsdale, A new gas permeameter for measuring the permeability of mortar and concrete.Magazine of Concrete Research. 40 (1988) 177-182.

[18] A. Dinku, H.W. Reinhardt, Gas permeability coefficient of cover concrete as a performance control, Mater Strucuture. 30 (1997) 387 – 393.

[19] C. Tasdemir , Combined effects of mineral admixtures and curing conditions on the sorptivity coefficient of concrete, Cement and Concrete Research. 33 (2003) 1637 – 1642.

[20] P. K. Mehta, P. J. M. Monteiro, Concreto: estrutura, propriedades e materiais, Pini, São Paulo, 1994.

[21] A. M. Neville, Propriedades do concreto. Trad. Salvador E. Giamusso, Pini, São Paulo, 1997.